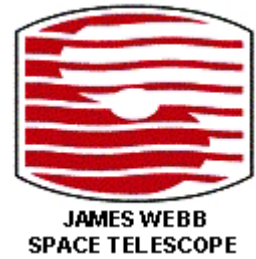


STSci-JWST-R-2002-0003

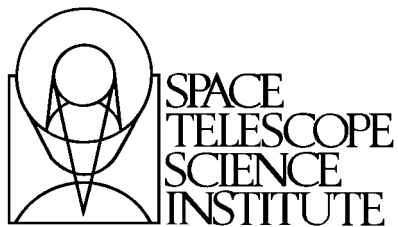


Space Telescope Science Institute  
James Webb Space Telescope Mission

---

Some Considerations on PSF Asymmetry and its  
Impact on the Measurement of Galaxy Shapes, 2002

Issue A



## REVISION HISTORY

ISSUE	DESCRIPTION	DATE
A	Initial Release	14-Nov-02

James Webb Space Telescope Mission

Some Considerations on PSF Asymmetry and its Impact on the  
Measurement of Galaxy Shapes

November 14, 2002

PREPARED BY: Stefano Casertano  
NAME

INS  
ORG.

\_\_\_\_\_  
SIGNATURE

11/14/2002  
DATE

\_\_\_\_\_  
NAME

\_\_\_\_\_  
ORG.

\_\_\_\_\_  
SIGNATURE

\_\_\_\_\_  
DATE

APPROVED BY:

\_\_\_\_\_  
SIGNATURE

\_\_\_\_\_  
NAME

\_\_\_\_\_  
TITLE

# Some Considerations on PSF Asymmetry and its Impact on the Measurement of Galaxy Shapes

Stefano Casertano, Space Telescope Science Institute

Version A: November 14, 2002

## Abstract

The anisotropy of the Point Spread Function (PSF) delivered by the James Webb Space Telescope (JWST) will affect the measurement of the shape of faint objects, such as those required for the mapping of the cosmic shear via weak lensing observations described in Program 003 in the JWST Design Reference Mission (DRM). We revisit the scientific impact of the PSF anisotropy in light of new observational results and theoretical developments on the analysis of faint objects, and introduce a simple criterion to help quantify the effect of the PSF on the measured shape of galaxies observed with JWST. We suggest two versions of a modified Level 2 requirement on the PSF anisotropy that would better represent our current understanding of the scientific requirements of weak lensing observations.

## 1 Introduction

The Level 2 Requirements for JWST include a set of specifications on the shape, size, and stability of the optical PSF delivered at the science focal plane by the combination of the telescope optics (the Optical Telescope Element, or OTE) and science instruments in the Integrated Science Instrument Module (ISIM). This PSF will presumably be monitored and stabilized by Wavefront Sensing and Control (WSC) activities and corresponding commanding of the primary mirror actuators, the focusing mechanism, and the fast steering mirror. Here we are concerned with motivating the requirements on the shape and stability of the PSF from a scientific standpoint, as well as providing a set of simple formulae for their calculation.

DRM Program 003, *Mapping the Dark Matter Distribution at High Redshift with NGST*, is especially sensitive to asymmetries of the PSF. According to the NGST Mission Simulator (NMS, Petro et al. 2001; see also <http://www.ngst.stsci.edu/studies/drmv2.3/>), this program represents about 20% of the total JWST core mission. The measurement of dark matter distribution in Program 003 based on weak gravitational lensing, which is the small distortion induced on the images of faint galaxies by foreground mass. Gravitational lensing is sensitive to the presence of mass regardless of its ability to emit radiation, and therefore offers a unique method to detect and measure the properties of dark matter. Recently, weak gravitational lensing has been used to study dark matter haloes around galaxies and the large-scale structure

of dark matter, with considerable success (Bacon et al 2001; van Waerbeke et al 2000, 2001; Maoli et al 2001; Wilson et al 2001; Casertano et al 2001, 2002).

Weak lensing studies require accurate measurements of the shapes of faint galaxies ( $I > 22$ ). Measuring faint, high-redshift galaxies is necessary to determine the growth of structure as a function of time. Even the best planned HST programs will probably be limited to  $z \sim 2$ , which will trace the growth of structure from  $z \sim 1.5$  to the present. With JWST, it will be possible to extend weak lensing studies to  $z \sim 4$  and beyond, thus probing the clustering of dark matter and the growth of galaxy haloes to  $z \sim 3$ .

Weak lensing measurements are by nature precision astronomy. Lensing distorts only slightly the image of each individual galaxy; its trace is in *correlated* distortions that can be measured on ensembles of thousands of galaxies. The amplitude of the shear due to lensing is measured by the quantity  $\gamma$  defined in the next Section, which is approximately half the ellipticity that would be induced in an intrinsically circular source; a lensing amplitude of, say, 2% induces an ellipticity of 0.04 in a circular galaxy. Correlated lensing distortions have been detected on angular scales ranging from  $20''$  to about  $15'$ , and decrease over this range from  $\gamma \sim 6\%$  to 1%. The predicted signal depends on the cosmology and on the growth of structure; to be minimally useful, the measurements obtained in the JWST DRM program must be able to discriminate between models that differ by 20–50% in their predictions (Jain and Seljak 1997, Barber et al. 2000), and thus need a relative precision of at least 10%, i.e., an uncertainty in  $\gamma$  of about 0.1%.

Unless carefully controlled and/or calibrated, PSF distortions can induce correlated distortions in galaxy images that mimic the effect of weak lensing, at levels comparable with the expected signal. Unlike the ellipticity induced by lensing, which is independent of the size of the galaxy, the effect of the PSF is more noticeable in galaxies of small angular size; the impact of PSF asymmetries on lensing measurements is thus largest for the smallest images. Unless PSF distortions and other instrumental effects are kept below about 10% of the expected signal, or 0.1% absolute distortion, they will dominate the uncertainties in the weak lensing measurement and hinder our ability to reach the scientific goals of the weak lensing DRM program. Therefore, the science requirement is that the impact of PSF asymmetries on the measured shape of galaxy images be understood and corrected to better than 0.1%, or one-tenth of the expected signal.

In this report we suggest a simplified, but easy-to-implement, method to estimate the distortion induced in galaxy images by PSF anisotropies. We cannot yet determine conclusively to what degree such distortions can be corrected; this ability depends critically on how well the PSF can be measured at any given time, either via wavefront sensing or through direct imaging, and on how well its properties are maintained between calibrations. In fact, correction of PSF-induced distortions need substantially more information than simply an estimate of their order of magnitude (Bernstein and Jarvis 2002).

The calculations we present here are significantly simplified with respect to what would be necessary in the course of conducting a scientific investigation of weak lensing. First, we consider the field dependence of the PSF only in the context of our ability to calibrate its anisotropy. PSF variations are likely to be very small on scales comparable to the sizes of the

target galaxies ( $< 1''$ ); however, variations on larger scales need to be taken into account when correcting for the effects of the PSF, and a PSF that varies significantly over the field of view is more difficult to calibrate. Second, we neglect pixelation issues, which are significant from a scientific point of view, but require a more careful consideration and only affect PSF issues indirectly. Third, we estimate the effect of PSF anisotropy on idealized, circular galaxies. Bernstein and Jarvis (2002) show that the effect of the PSF on non-circular galaxies can be readily estimated by the effect on circular galaxies; while the effect of the PSF does depend on the light distribution within the galaxy, we can obtain most of the necessary information by assuming a Gaussian light distribution for the galaxy. A more complete discussion of PSF effects and their correction would require applying the Bernstein and Jarvis formalism, or equivalent results from other authors, and is beyond the scope of this discussion. Finally, we do not attempt to define ‘optimal’ measurements for the purpose of any specific science program. For example, it is possible that fitting methods could yield somewhat improved performance compared to the weighted integrals described here. On the other hand, the performance of fitting methods is more difficult to quantify, and can be adversely affected by even small imperfections in our knowledge of the PSF. Lacking a detailed set of prescriptions on the quality of the PSF model at any given time, the analysis of fitting methods is of necessity limited at this time.

## 2 The effect of weak lensing

Weak lensing shears the image of a galaxy by stretching it by different amounts along perpendicular axes. As a result of the shear, a circular galaxy image will thus become an ellipse; an elliptical image will be distorted into a different ellipse, in general with a different orientation of the major and minor axes. In a given local  $(x, y)$  coordinate system, the lensing shear can be described by two components:  $\gamma_1$  is the ellipticity induced along the  $x$  axis, and  $\gamma_2$  the ellipticity induced along the positive  $(xy)$  diagonal. Thus a circular galaxy image will become an ellipse with the major axis in the  $x$  direction if  $\gamma_1 > 0$ ,  $\gamma_2 = 0$ ; with the major axis along the diagonal if  $\gamma_1 = 0$ ,  $\gamma_2 > 0$ .

The detection of a weak lensing signal is based on the correlation of the distortion induced in a large number of galaxy images. The true (unlensed) shape of an individual galaxy image is not known, and therefore its measured shape cannot be used to determine the weak lensing shear directly. However, if a large number of galaxies is subject to the same—or similar—shear, its effect is statistically detectable. Various methods have been suggested to carry out this statistical analysis (Schneider and Seitz 1995, Bacon et al 2001, Casertano et al 2001, Bernstein and Jarvis 2002); although the details differ, they all amount to measuring the correlation of the ellipticity measured for a large number of spatially contiguous galaxies. Typically, such methods cannot reliably measure the shear  $(\gamma_1, \gamma_2)$  at or around a given line of sight, but they *can* measure statistically the distribution of the total shear,  $\gamma = \sqrt{\gamma_1^2 + \gamma_2^2}$ , from the degree to which galaxy ellipticities are correlated in a region of a given size. Measurements based on ground-based data indicate values  $\gamma \sim 1\%$  to  $3\%$ , on scales ranging from  $15'$  to  $1'$ . Early HST measurements show that  $\gamma \sim 4\%$  to  $6\%$  on smaller angular scales, down to  $10''$ .

Cosmic shear is expected to increase with redshift in a way that depends on cosmology, via both the geometry of the universe and the history of structure formation (Jain and Seljak 1997, Barber et al. 2000). Detection of cosmic shear separately for galaxies in different redshift slices will thus provide strong constraints on cosmology. With JWST, it should be possible to detect separate lensing signals from galaxies at redshift as low as  $z \sim 1$  and as high as  $z > 4$ , thus tracing a clear picture of the evolution of structure in the dark matter component. Such measurements require the ability to measure shear as small as  $\gamma \sim 1\%$  with a fractional accuracy ( $1-\sigma$ ) of 10% or better, and therefore it is important that systematic errors in the cosmic shear measurement, which will be due primarily to uncorrected PSF effects, remain below 0.1%.

### 3 The effect of the PSF

Weak lensing measurements are based on the apparent shape of galaxy images on the sky. The optical/detector train introduces several distortions in each galaxy image. First, the images are broadened by convolution with the PSF, which effectively dilutes the effect of the lensing shear. Second, any asymmetry of the PSF results in an asymmetry of the detected image; such asymmetries are likely to be correlated for nearby galaxies, and therefore effectively mimic lensing shear. Third, the detected image is pixelated, which a) further softens the image by convolution with the pixel response function, and b) introduces aliasing unless the image is properly sampled. Fourth, the detection process introduces noise in the image, which limits the accuracy with which the shape of each galaxy image can be measured. All of these effects are important in practice; the first two can be expressed in actual requirements on the PSF properties, while the latter two determine how best to carry out effective measurements of galaxy shapes.

In the following, we will consider primarily the artificial image distortion introduced by the anisotropy of the PSF, which is the subject of the requirement under examination. Any measurement of the lensing shear also requires the PSF dilution effect to be well-characterized and corrected with sufficient accuracy, but this topic will be considered in a separate document. Pixelation effects, while important, appear to be less problematic in practice.

### 4 Measuring asymmetries: some definitions

A common method to measure shape and asymmetry of a light distribution  $I(x, y)$ —which can be either a galaxy or the PSF—is to form its first- and second-order moments with an optional weight  $w(x, y)$ , and consider the second-order moment along specific axes. For simplicity, we assume that the light distribution and the weight are both everywhere non-negative.

The first-order moment is the vector:

$$\bar{x} = \int xw(x, y)I(x, y)dxdy / \int w(x, y)I(x, y)dxdy \quad (1)$$

$$\bar{y} = \int y w(x, y) I(x, y) dx dy \bigg/ \int w(x, y) I(x, y) dx dy \quad (2)$$

The second-order moment is the tensor:

$$I_{uv} = \int (u - \bar{u})(v - \bar{v}) w(x, y) I(x, y) dx dy \bigg/ \int w(x, y) I(x, y) dx dy \quad (3)$$

where each of  $u, v$  can be either  $x$  or  $y$ . The second-order moment along a direction  $\xi = x \cos(\theta) + y \sin(\theta)$  is defined as:

$$I_{\xi\xi} \equiv \int (\xi - \bar{\xi})(\xi - \bar{\xi}) w(x, y) I(x, y) dx dy \bigg/ \int w(x, y) I(x, y) dx dy \quad (4)$$

where  $\bar{\xi} = \bar{x} \cos(\theta) + \bar{y} \sin(\theta)$ .

The tensor can be written in the form of the  $2 \times 2$  symmetric matrix:

$$\begin{pmatrix} I_{xx} & I_{xy} \\ I_{xy} & I_{yy} \end{pmatrix} \quad (5)$$

The elements of this matrix depend on the coordinate system chosen. It is useful to form some quantities that are coordinate-independent. We define the total second-order moment as the *trace* of the tensor:

$$I_{total} = I_{xx} + I_{yy} . \quad (6)$$

It is readily verified that this quantity is unchanged for any rotation of the coordinate system  $x' = x \cos(\theta) + y \sin(\theta)$ ,  $y' = -x \sin(\theta) + y \cos(\theta)$ . We also define the ellipticity  $\chi$  of the light distribution as the quantity:

$$\chi = \frac{\sqrt{(I_{xx} - I_{yy})^2 + 4I_{xy}^2}}{(I_{xx} + I_{yy})} \quad (7)$$

Simple algebra shows that the second-order moment in an arbitrary direction  $\xi = x \cos(\theta) + y \sin(\theta)$  can be expressed as:

$$I_{\xi\xi} = (I_{total}/2) [1 + \chi \cos 2(\theta - \theta_0)] \quad (8)$$

where  $\theta_0$  is the position angle of the major axis of the ellipse; obviously this quantity is maximum at  $\theta = \theta_0$ , minimum at  $\theta = \theta_0 + \pi/2$ . It is also apparent that, for any orthogonal pair of axes  $(\xi, \eta)$ , the quantity  $I_{\xi\xi} + I_{\eta\eta}$  is constant.

The maximum and minimum second-order moments are  $I_{MM} = I_{total}(1 + \chi)/2$ ,  $I_{mm} = I_{total}(1 - \chi)/2$  respectively. The ellipticity  $\chi$  can thus be expressed as

$$\chi = \frac{I_{MM} - I_{mm}}{I_{MM} + I_{mm}} \quad (9)$$

In geometric terms, the light distribution can be described by an ellipse with first- and second-order moments corresponding to those of the light distribution. Conventionally, the

ellipse is centered at  $(\bar{x}, \bar{y})$ , the first-order moments, and in any direction  $\xi$ , the elliptic radius equals the square root of the second-order moment  $I_{\xi\xi}$  in that direction. Thus the major axis of the ellipse is aligned with the direction of the maximum second-order moment, and its square equals  $I_{MM}$ ; the minor axis is aligned with the direction of the minimum second-order moment, and its square equals  $I_{mm}$ . The axis ratio  $b/a$  of the ellipse is related to the ellipticity  $\chi$  of the second-order moment by:

$$\chi = \frac{1 - b^2/a^2}{1 + b^2/a^2} \quad (10)$$

Note that all of the above properties are formally true for any non-negative light distribution  $I(x, y)$  and weight  $w(x, y)$ , as long as the appropriate integrals converge. In other words, they depend only on the definition of image moments, and not on the properties of the PSF or of the galaxy image.

## 5 Galaxy shape and PSF—the unweighted version

A very simple method to measure the shape and orientation of galaxy images is to use the axis ratio and position angle as determined by the second order moments of the image intensity  $I(x, y)$ . This method can be readily applied to observed images—modulo pixelation—and can yield a reasonable measurement of the image parameters. In terms of the definitions above, the ellipticity of the galaxy is defined as:

$$e_I = \frac{I_{MM} - I_{mm}}{I_{MM} + I_{mm}} \quad (11)$$

A not-so-obvious advantage of using second-order moments of the image intensity is that the effect of convolution with the PSF is very easily computed. Assume that the galaxy image has a true intensity  $I(x, y)$  before imaging, and that the imaging process effects a convolution with the PSF  $P(x, y)$  so that the observed image is:

$$O(x, y) = \int I(x', y') P(x - x', y - y') dx' dy' \quad (12)$$

Then it can be easily shown that the second order moments of the observed image,  $O_{xx}, O_{yy}, O_{xy}$  are simply the sum of the second-order moments of the true image  $I_{xx}, I_{yy}, I_{xy}$  and of the corresponding moments of the PSF  $P_{xx}, P_{yy}, P_{xy}$ . The impact of the PSF on the measured image shape is thus easy to determine theoretically.

Consider for example an intrinsically circular galaxy, with  $I_{xx} = I_{yy} = I$ ,  $I_{xy} = 0$ . Then the major and minor axes of the observed image  $O$  will be aligned with those of the PSF, and we will have  $O_{MM} = P_{MM} + I$ ,  $O_{mm} = P_{mm} + I$ . The observed ellipticity is:

$$e_O = \frac{O_{MM} - O_{mm}}{O_{MM} + O_{mm}} = \chi \cdot P_{total} / (P_{total} + I_{total}) \quad (13)$$

In other words, the observed ellipticity for an intrinsically circular galaxy is the ellipticity of the PSF, diluted by the (square of the) size of the PSF with respect to the observed size of the galaxy.

The maximum spurious ellipticity thus induced in a marginally resolved galaxy—i.e., a galaxy with  $I_{total} \sim P_{total}$ —is thus one-half the PSF anisotropy  $\chi$  defined in Section 4. The anisotropy induced in larger galaxies decreases by the square of the size of the galaxy relative to the PSF, as  $I_{total} \propto (size)^2$ . This effect is included in the PSF anisotropy condition of Equation 24 in the next Section.

## 6 Limitations of unweighted measurements; using weighted moments.

In reality, the simple description above cannot be applied to real data. First, the formula expressing the impact of a PSF only applies for an infinite integration domain, and in practice all integrations on real data are limited by the presence of other objects, requiring the use of an appropriate window function. Second, it is easy to show that the unweighted image moments are not the optimal image statistic in the presence of noise background. Since we wish to extend the measurements to galaxies as faint as practical, the use of weights that optimize the measurement of the signal-to-noise ratio (S/N) is desirable. Third, the second-order moments of the PSF may converge slowly—or not at all—causing an inordinately large contribution of the PSF to the image shape. In practice, a condition such as that indicated at the end of the previous section may be extremely difficult to satisfy for any realistic PSF without some additional, and artificial, large-angle cutoff.

Various algorithms have been proposed to improve the quality of image shape measurements and reduce their dependence on large-angle PSF properties (Kaiser et al 1995, Griffiths et al. 1996, Fischer and Tyson 1997, Kuijken 1999, Kaiser 2000, Casertano et al. 2001, Bernstein and Jarvis 2002). The quality of the results is expected to be similar for any of these methods; for the purpose of this discussion, we consider the approach used by Kaiser et al (1995) and Bernstein and Jarvis (2002), who use weighted moments with a symmetric Gaussian weight with the size matched to that of the galaxy image itself.

Unfortunately, the anisotropy induced in the galaxy moments by the PSF anisotropy cannot in general be expressed in closed form, even in the simplified case of a Gaussian galaxy image. Bernstein and Jarvis (2002) illustrate an orthogonal functions expansion that can be used to characterize the impact of the PSF on a galaxy image, but its practical use requires very detailed information on the PSF. For now, we *assume* that the anisotropy induced in the image of a circular galaxy of width  $\sigma$  is expressed by a formula analogous to (13) above:

$$e_O \approx \chi \cdot P_{total} / (P_{total} + I_{total}) \quad (14)$$

where however the PSF anisotropy  $\chi$  and size (related to  $P_{total}$ ) are defined by the second-order moments of the PSF weighted with a Gaussian with size comparable to the observed image size. This formula is exact for unweighted moments, and is correct to within a factor of 2 if all functions involved are Gaussians. In tests with realistic PSFs, this expression appears to be a conservative estimate of the anisotropy induced on a smooth galaxy, by a factor of 2 to 4. We therefore adopt Equation 14 as a useful, conservative approximation for the anisotropy

induced by a non-symmetric PSF under fairly general circumstances. The implications of this assumption are made explicit in the next Section.

## 7 A tentative PSF anisotropy criterion for lensing measurements

Consider a circular galaxy with observed half-light radius  $r_{half}$ . We define its first- and second-order moments using a Gaussian weight with the same half-light radius, which has one-dimensional dispersion  $\sigma = r_{half}/\sqrt{2 \ln 2}$ . We use the same weight function for the moments of the PSF, which are thus defined as:

$$M(\sigma) = \int P(x, y) \exp\left(-\frac{x^2 + y^2}{2\sigma^2}\right) dx dy \quad (15)$$

$$\bar{x} \equiv P_x(\sigma) = (1/M) \int x P(x, y) \exp\left(-\frac{x^2 + y^2}{2\sigma^2}\right) dx dy \quad (16)$$

$$\bar{y} \equiv P_y(\sigma) = (1/M) \int y P(x, y) \exp\left(-\frac{x^2 + y^2}{2\sigma^2}\right) dx dy \quad (17)$$

$$P_{xx}(\sigma) = (1/M) \int (x - \bar{x})^2 P(x, y) \exp\left(-\frac{x^2 + y^2}{2\sigma^2}\right) dx dy \quad (18)$$

$$P_{xy}(\sigma) = (1/M) \int (x - \bar{x})(y - \bar{y}) P(x, y) \exp\left(-\frac{x^2 + y^2}{2\sigma^2}\right) dx dy \quad (19)$$

$$P_{yy}(\sigma) = (1/M) \int (y - \bar{y})^2 P(x, y) \exp\left(-\frac{x^2 + y^2}{2\sigma^2}\right) dx dy. \quad (20)$$

Each of these integrals can be cut off at a radial distance  $\sim 5\sigma$  or at  $5''$ , whichever is smaller.

The anisotropy  $\chi(\sigma)$  of the PSF can be defined as:

$$\chi(\sigma) = \frac{\sqrt{(P_{xx} - P_{yy})^2 + 4P_{xy}^2}}{(P_{xx} + P_{yy})} \quad (21)$$

where each of the second-order moments is a function of  $\sigma$ .

The weighted anisotropy induced on a circular galaxy image of apparent size  $\sigma$  by the PSF is estimated to be:

$$e_O \sim \chi_{eff}(\sigma) \equiv \chi(\sigma) \cdot P_{total}(\sigma) / [2\sigma^2 + P_{total}(\sigma)]. \quad (22)$$

where we introduce the ‘effective’ PSF anisotropy  $\chi_{eff}(\sigma)$  for the observation of a galaxy of size  $\sigma$  as the PSF anisotropy weighted with weight scale  $\sigma$ , and diluted by the size of the galaxy, and  $\chi(\sigma)$  and  $P_{total}(\sigma)$  are the appropriate combinations of second-order moments of the PSF using the weight function  $\exp(-\frac{x^2+y^2}{2\sigma^2})$ . Here and elsewhere,  $\sigma$  is defined as the dispersion

of the Gaussian that best represents the light distribution of the galaxy, and approximately equals its half-light radius; the exact definition of  $\sigma$  is not critical.

We can now introduce the ‘maximum effective anisotropy’  $\chi_{\max}$  as the largest effective anisotropy induced by the PSF over the range of galaxy sizes of interest, which we estimate to be the range  $0.1''$  to  $3''$ . Thus:

$$\chi_{\max} \equiv \max_{0.1'' < \sigma < 3''} [\chi_{eff}(\sigma)] . \quad (23)$$

The effective anisotropy explicitly takes into account the dilution of the PSF anisotropy due to galaxy size and weighting.

The requirement for weak lensing measurements (Section 2) is that the effective anisotropy induced on galaxy images, *after correcting for the known PSF*, be less than 0.1%. If no additional knowledge of the PSF is available, a *sufficient* condition is:

$$\chi_{\max} < 0.1\% . \quad (24)$$

In practice, if the PSF can be characterized to about 10–20%, a practical limit may well be  $\chi_{\max} < 0.5\%–1\%$ .

## 8 Some estimates on a model PSF

In order to gain some understanding of the meaning of the effective anisotropy  $\chi_{eff}$  under somewhat realistic circumstances, we have measured the weighted second-order moments of a number of model PSFs computed by Green (2002) for a primary mirror composed of 36 hexagonal segments, including intersegment gaps and secondary mirror obscuration. The ‘ideal’ configuration, used for Figure 1, reflects the PSF for a perfectly aligned and figured primary; only the aberrations inherent in the optical design are included. The realistic PSFs used for Figures 2 and 3 include random amounts of figure errors and misalignments between segments, in such amounts that the configuration meets the overall Strehl ratio and encircled energy requirements. The total diameter of the system is 6.5 m.

### 8.1 Diffraction-limited performance

Figure 1 shows the second-order moments and the anisotropy of the central PSF for the ideal optical configuration described above, through a broadband filter centered at  $2 \mu\text{m}$ . The results are indicative of the performance of a diffraction-limited JWST at  $2 \mu\text{m}$ . The following features are worth noting:

1. The weighted moments increase significantly as the scale of the weight increases. This is a good indication that unweighted moments are poorly defined for a realistic PSF.
2. The intrinsic PSF anisotropy also increases as the scale increases. This suggests that the PSF halo may be intrinsically more asymmetric than its core. The PSF halo has less impact for small galaxies, but it can cause significant distortion in the image of larger galaxies.

Ideal PSF at  $2\mu\text{m}$  – 36 hexagonal segments

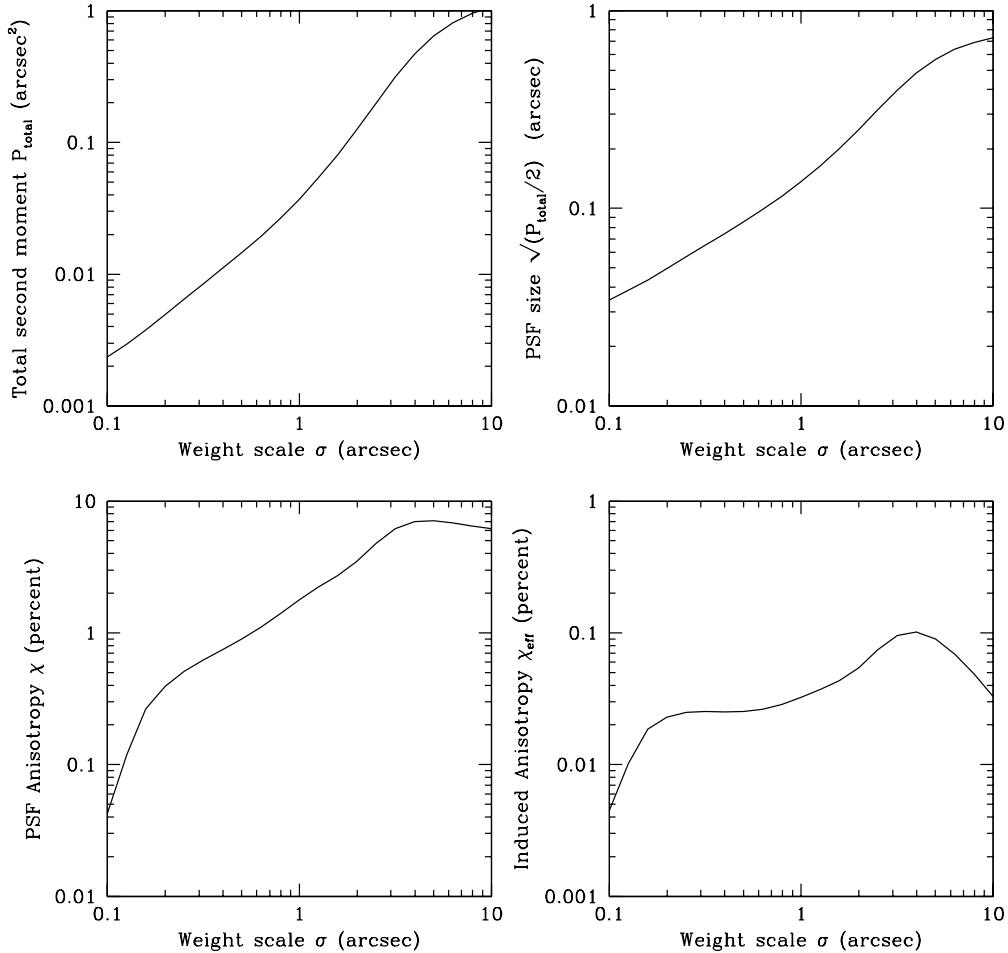


Figure 1: Properties of an ideal PSF produced by 36 hexagonal mirrors in a Keck-like configuration, at a wavelength of  $2\mu\text{m}$ . Top left: total second order moment. Top right: Size estimated from the second order moment; this size estimate would equal the rms dispersion for an unweighted Gaussian PSF. Bottom left: weighted PSF anisotropy  $\chi$  (eq. 21). Bottom right: Effective anisotropy  $\chi_{\text{eff}}$  (eq. 22) for a galaxy of size  $\sigma$ , after dilution with the galaxy size.

3. The PSF anisotropy condition (equation 24) is readily satisfied at  $2\mu\text{m}$  on scales up to  $2\text{--}3''$ . On larger scales, the anisotropic halo of the PSF can introduce a significant distortion, and—unless the PSF can be measured accurately—galaxies larger than about  $2''$  may not make good targets for weak lensing measurements. As discussed previously, most of the interesting signal is expected to come from galaxies smaller than  $1''$ ; in any event, galaxies of larger angular size can be effectively studied with ground-based telescopes.

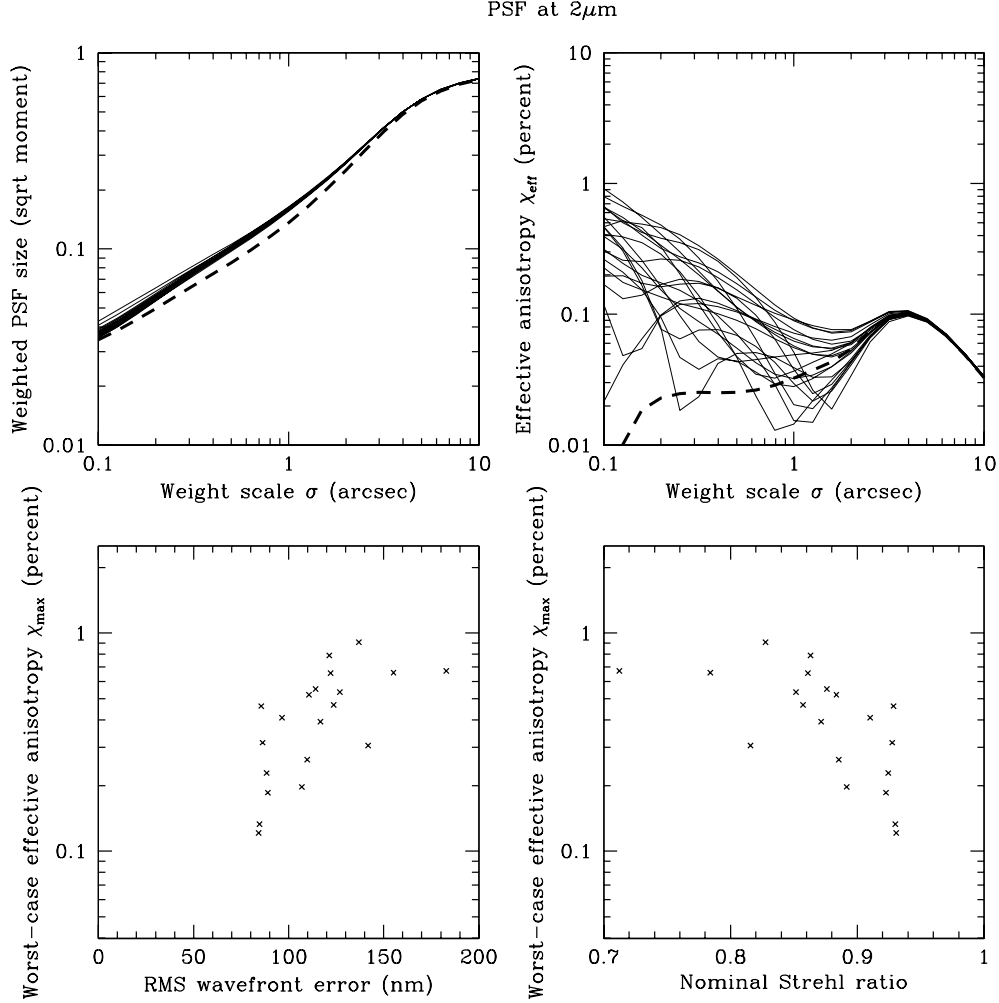


Figure 2: Properties of  $2\mu\text{m}$  PSFs with the same configuration as in Fig. 1, but with ‘realistic’ wavefront errors. The top left panel shows the apparent size of the PSF from the second order moments, and the top right plot shows the effective anisotropy induced on galaxies of different sizes. The bottom two panels show the worst-case induced anisotropy vs. two PSF quality parameters, the rms wavefront error and the nominal Strehl ratio (without the effect of finite pixel size). In both cases, the PSF anisotropy is somewhat correlated with PSF quality; however, PSFs that are acceptable in terms of wavefront error and Strehl ratio can have anisotropies that exceed the criterion of Equation 24 by a factor up to 10. The heavy dashed lines refer to the diffraction-limited case of Fig. 1.

Nonetheless, it appears from Figure 1 that the condition  $\chi_{eff} < 0.1\%$  is easily satisfied for a *perfect* PSF even if produced from a combination of hexagonal apertures. The key question is how well the PSF will be maintained in practice, and how stable its characteristics will remain between wavefront sensing measurements. We start to address some of these points below.

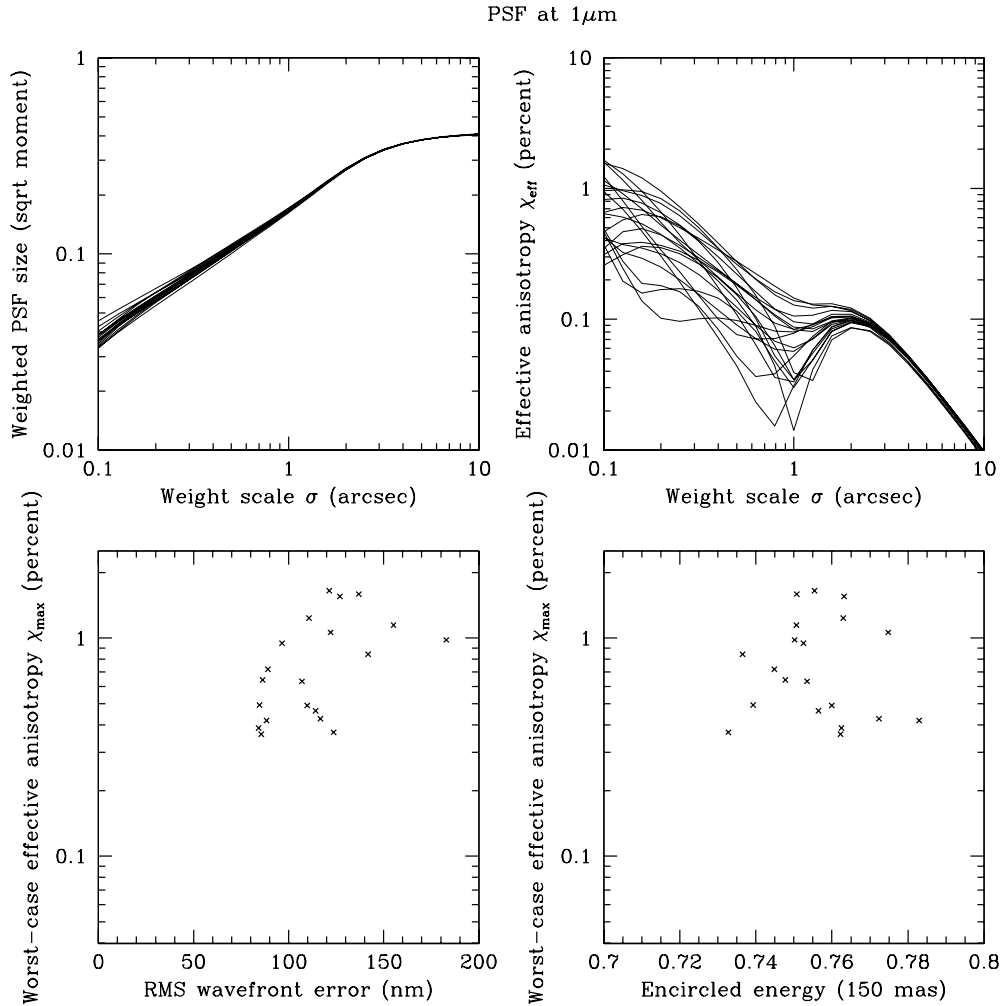


Figure 3: Properties of the PSFs in Figure 2, but observed at  $1\mu\text{m}$ . The same wavefront errors at a shorter wavelength with ‘realistic’ wavefront errors. The top left panel shows the apparent size of the PSF from the second order moments, and the top right plot shows the effective anisotropy induced on galaxies of different sizes. Although smaller than at  $2\mu\text{m}$ , the PSF is intrinsically more asymmetric, resulting in overall higher induced anisotropy for small galaxies ( $< 0.5''$ ). The bottom two panels show the worst-case induced anisotropy vs. the same wavefront error used in Fig. 1 and the 150 mas encircled energy. There is some indication of a correlation between nominal PSF quality and induced anisotropy, but less strong than at  $2\mu\text{m}$ .

## 8.2 Expected performance under wavefront control

During normal operations, the PSF of JWST will be controlled by appropriate wavefront sensing and control procedures. These will maintain the PSF quality within well-defined specifications, but—due to temporal variability, the limited amount of calibration time available

and the difficulty of obtaining a perfect correction—residual PSF errors will remain. We have considered 20 PSFs that may arise with realistic amounts of uncorrected wavefront error, due to small figure errors of individual segments and misalignments between segments (Green 2002). The random imperfections are such that each PSF meets the Level 2 requirements on Strehl ratio at  $2\mu\text{m}$  and on encircled energy at  $1\mu\text{m}$ .

The properties of the resulting PSFs at  $2\mu\text{m}$  are shown in Figure 2. The top left panel indicates the PSF size as measured from the second-order moments, and the top right panel the effective anisotropy  $\chi_{eff}$  induced on round galaxies as a function of their size. In both cases the heavy dashed line refers to the diffraction-limited case. Unlike the case of the ideal PSF, the core itself can be significantly asymmetric, and the largest effective anisotropy is often seen for the smallest galaxy sizes. The two bottom panels show how the induced anisotropy at  $2\mu\text{m}$  correlates with two quantities that can be used to measure the PSF quality: the rms wavefront error (left) and the nominal Strehl ratio. Both quantities correlate with the induced anisotropy, and therefore can be used to some extent to track the performance of the PSF for weak lensing studies. However, even for PSFs that are acceptable in terms of wavefront error or Strehl ratio, the induced anisotropy can exceed the nominal requirement (eq. 24) by as much as a factor 10. Therefore weak lensing measurements at  $2\mu\text{m}$  require that PSF-induced asymmetries be calibrated and removed at the level of 10 percent or better.

Figure 3 shows the properties of the same PSFs at  $1\mu\text{m}$ . The panels are as in Figure 2, but we use the encircled energy at 150 mas in place of the Strehl ratio, which is poorly constrained at these short wavelengths. The effective anisotropy shows a weak correlation with rms wavefront error, and no significant correlation with encircled energy. Despite the smaller PSF compared to  $2\mu\text{m}$ , the increased anisotropy causes an even larger distortion at such wavelengths, especially for small galaxies ( $< 0.5''$ ). The worst-case induced anisotropy  $\chi_{max}$  exceeds the requirement of equation 24 by as much as a factor 15. Weak lensing measurements at  $1\mu\text{m}$  thus require that the PSF anisotropy be characterized and corrected for at the level of 7 percent or better.

## 9 The current Level 2 Requirement on PSF anisotropy

The current Level 2 requirement on PSF anisotropy reads: *‘The square root of the combined second moments of the square of the point spread function (PSF) in any two orthogonal dimensions in the science focal plane shall differ by less than 5 percent RMS at  $2\mu\text{m}$  between OTE re-calibrations.’*

This definition is based on the moments of the *square* of the PSF, which is equivalent to using the PSF itself as the weight  $w$  in the definitions of Section 4. With that proviso, the quantity used in this definition is the difference of the square roots of second order moments in orthogonal directions, which can be expressed using Equation 8 as:

$$\sqrt{I_{\xi\xi}} - \sqrt{I_{\eta\eta}} = \sqrt{\frac{I_{total}}{2}} \left[ \sqrt{1 + \chi \cos(2(\theta - \theta_0))} - \sqrt{1 - \chi \cos(2(\theta - \theta_0))} \right] \quad (25)$$

The maximum of this quantity as  $\theta$  varies is:

$$\max_{\theta} \left( \sqrt{I_{\xi\xi}} - \sqrt{I_{\eta\eta}} \right) = \sqrt{\frac{I_{total}}{2}} \left[ \sqrt{1+\chi} - \sqrt{1-\chi} \right] \quad (26)$$

and in order for the quantity to differ by ‘less than 5 per cent’ (of the typical value  $\sqrt{I_{total}/2}$ ), we must have:

$$\sqrt{1+\chi} - \sqrt{1-\chi} < 0.05 \quad (27)$$

which in turn is satisfied if  $\chi < 0.05$  (actually 0.04998).

Therefore the current Level 2 Requirement is satisfied if the anisotropy  $\chi$  of the PSF, as defined in Section 4, using as weight the PSF itself, is less than 5%. However, as discussed elsewhere in this report, this requirement is not optimally matched to the needs to the weak lensing programs, which 1) require much better precision than 5%, 2) are based on weighting the PSF by the light distribution of a typical galaxy, not the PSF itself, and 3) should take into account the correctability of the PSF itself. In fact, the current Level 2 requirement is violated by several of the PSFs considered in the Section 8.2, which have PSF-squared anisotropies of up to 7%. As a consequence, the current Level 2 anisotropy requirement does not ensure that core JWST science can be carried out, and furthermore may be difficult to satisfy with the level of wavefront control that is currently envisioned.

## 10 Proposed requirements on PSF anisotropy

The expected scientific impact of JWST on cosmology and dark matter measurements via weak lensing can only be ensured if the systematic effect of PSF anisotropy on the measurement of galaxy shapes is controlled to better than 0.1%. This means that either the PSF-induced image anisotropy is kept below 0.1% via high-quality wavefront sensing and control, or the effect of the PSF can be corrected to better than 0.1% via a careful program of calibration and analysis. Of course, intermediate solutions, such as limiting the PSF anisotropy to a lesser extent than demanded by the first option, and correcting the smaller residual induced anisotropy, are also possible.

So far, we have presented a quantitative description of the implications of the first option, controlling the PSF anisotropy. We have not discussed in detail what requirements, if any, need to be imposed to ensure that the calibration of the PSF-induced anisotropy can achieve the required precision. This calibration typically requires careful measurement of the PSF itself, e.g., from a collection of point sources in either science or calibration images, as well as analysis tools that can compensate for known PSF anisotropies. Such tools exist already (Kaiser et al. 1995, Bernstein and Jarvis 2002), but have been applied to space-based images only to a limited extent. Their effectiveness has been studied best for typical ground-based images, in which the impact of the PSF on the shape of each source is large since target sources are poorly resolved, but many point sources are available for PSF calibration within each image. In the conditions we expect to prevail in space-based images, images are typically well-resolved, thus

reducing the impact of PSF distortions, but the number of point sources available for PSF measurement is small.

Primarily, the quality of the PSF calibration depends on how well the PSF itself can be characterized, which in turn depends on its spatial and temporal variations. For example, consider a PSF calibration program based on observations of point sources. If the PSF varies from image to image, its calibration can only be based on point sources observed in the same image as the desired targets; if the PSF varies over a scale of  $1'$ , then only point sources within that  $1' \times 1'$  region can be used. Typically, we expect a minimum of about 10–20 stars brighter than  $K \sim 22$  in the NIRCcam field of view; such stars will be detected with a S/N of several hundred in broad-band observations at  $2 \mu\text{m}$ . As long as the PSF is constant over the field of view, measuring  $\sim 10$  stars may suffice to effect the correction to the PSF-induced anisotropy with 10% fidelity, which in turn would be enough to relax the 0.1% requirement on the PSF anisotropy by a factor of about 10, to 1%—a far easier requirement to meet for the hardware.

We emphasize, however, that these relations are for the moment qualitative and require a more detailed investigation of 1) the type and scale of PSF variations within the field of view and from image to image, 2) the type of PSF calibration programs that can be carried out, and 3) the algorithms that can be used to convert high-S/N measurements of the PSF to corrections of their impact on measured source shapes.

With those caveats, we suggest two options for possible PSF requirements that are expected to be sufficient to ensure scientifically useful weak lensing measurements with JWST: controlling the anisotropy, or ensuring that its effects can be calibrated.

### 10.1 Option 1: Controlling the anisotropy

On the basis of the discussion presented here, a Level 2 Requirement on the anisotropy of the JWST PSF that would enable meaningful, scientifically valid weak lensing measurements would be as follows:

The maximum effective anisotropy of the JWST PSF at  $2\mu\text{m}$ , weighted with a circular Gaussian of width  $\sigma$  ranging from  $0.1''$  to  $1''$ , shall not exceed 0.1% when averaged in quadrature over the field of view of the near-infrared camera and over the time interval between successive wavefront sensing measurements.

For the purpose of this proposed Requirement, the following definitions and conventions hold:

1. The ‘PSF weighted with a circular Gaussian of width  $\sigma$ ’ is the function  $P(x, y)$  defined as:

$$P(x, y) = PSF(x, y) \times \frac{1}{2\pi\sigma^2} \exp \left[ -\frac{(x - x_0)^2 + (y - y_0)^2}{2\sigma^2} \right]$$

where  $(x, y)$  are rectilinear focal plane coordinates expressed in seconds of arc,  $PSF(x, y)$  is the unweighted PSF at the detector, and  $(x_0, y_0)$  is the location of its peak.

2. The anisotropy  $\chi$  of a function of focal plane coordinates  $P(x, y)$  is defined from the second order moments of the function as:

$$\chi = \frac{\sqrt{(P_{xx} - P_{yy})^2 + 4P_{xy}^2}}{P_{xx} + P_{yy}}$$

Note that the anisotropy thus defined is independent of the choice of the orientation of the coordinate system.

3. The ‘effective anisotropy’  $\chi_{eff}$  is defined as in Equation 22:

$$\chi_{eff}(\sigma) \equiv \chi(\sigma) \cdot \frac{P_{xx}(\sigma) + P_{yy}(\sigma)}{2\sigma^2 + P_{xx}(\sigma) + P_{yy}(\sigma)}$$

where  $P_{xx}(\sigma), P_{yy}(\sigma)$  are the second-order moments of the PSF weighted with a circular Gaussian of width  $\sigma$ .

4. All integrals involving a weighted PSF can be cut off at the smaller of  $5\sigma$  or  $5''$  from the peak of the PSF.

Note that the requirement above does not take into account the correction for the PSF dilution itself. In this report we have focused on spurious anisotropies induced by the non-circularity of the PSF. However, even a perfectly circular PSF introduces a bias in weak lensing measurements, since the distortion of a galaxy image is affected by the size of the PSF itself. This effect, dominant in ground-based lensing measurements, is expected to be small in space-based measurements, where the PSF is narrower than a typical galaxy image. Nonetheless, some requirement on the PSF size and its stability is necessary to insure that uncertainties in the PSF dilution do not excessively degrade weak lensing measurements. It is not expected that dilution constraints will be especially onerous to achieve.

## 10.2 Option 2: Calibrating PSF-induced anisotropy

The alternative requirement to ensure that the PSF-induced anisotropy can be calibrated is more difficult to formulate, primarily because of the current lack of knowledge of the expected PSF variability and of the quantitative aspects of PSF corrections in the low PSF regime.

If we *assume* that a small number of PSFs, of order 10, detected with S/N exceeding 100 are sufficient to characterize their induced anisotropy on galaxies of size ranging from  $0.1''$  to  $1''$  with a fidelity of 10%, then a sufficient set of alternate Level 2 requirements could read:

- 1) The maximum effective anisotropy of the JWST PSF at  $2\mu\text{m}$ , weighted with a circular Gaussian of width  $\sigma$  ranging from  $0.1''$  to  $1''$ , shall not exceed 1% when averaged in quadrature over the field of view of the near-infrared camera and over the time interval between successive wavefront sensing measurements.

2) The rms variation of each component of the effective anisotropy of the JWST PSF at  $2\mu\text{m}$ , weighted with a circular Gaussian of width  $\sigma$  between  $0.1''$  and  $1''$ , shall not exceed 0.1% over the field of view of the near-infrared camera at any given time.

The same definitions as in Section 10.1 apply. In addition, we introduce the two components of the anisotropy,  $\chi_1$  and  $\chi_2$ , and of the effective anisotropy,  $\chi_{1,eff}$  and  $\chi_{2,eff}$ , defined as follows:

$$\chi_1(\sigma) = \frac{P_{xx} - P_{yy}}{P_{xx} + P_{yy}}; \quad \chi_2(\sigma) = \frac{2P_{xy}}{P_{xx} + P_{yy}}$$

$$\chi_{1,eff}(\sigma) \equiv \chi_1(\sigma) \cdot \frac{P_{xx} + P_{yy}}{2\sigma^2 + P_{xx} + P_{yy}}; \quad \chi_{2,eff}(\sigma) \equiv \chi_2(\sigma) \cdot \frac{P_{xx} + P_{yy}}{2\sigma^2 + P_{xx} + P_{yy}}$$

where  $P_{xx}(\sigma), P_{yy}(\sigma)$  are the same quantities used in Section 10.1.

The second requirement above is to be interpreted in the sense that, for a given value of  $\sigma$ , the effective anisotropy is constant to 0.1% rms over the entire image. Note that the effective anisotropy *is* expected to vary significantly as  $\sigma$  varies over the specified range.

The sense of the second requirement is to ensure that, even if the PSF shape is not symmetric, its asymmetry is constant over the field of view, so that its calibration is possible. The present version focuses on the case in which the PSF is spatially constant but temporally variable; a more complete version of the second requirement would allow for a combined spatial and temporal stability such that calibration of the PSF remains possible.

### 10.3 Other calibration possibilities

The view of PSF calibration expressed above is somewhat simplistic. Other calibration procedures can be used to augment our understanding of the PSF properties and of its impact on measured galaxy shapes. For example, the same field can be observed at different times, dither positions, and roll angles; comparing the shapes measured for the same galaxy in different images will help determine what the true (lensing-distorted) shape of the galaxy is. Furthermore, it is possible to trade temporal for spatial stability. If the PSF is *not* constant to the required degree over the field of view, but its spatial variations follow a well-defined pattern that remains constant in time, then its calibration may be possible, either by comparing the point sources and galaxies measured in different images, or by observing star-rich calibration fields. Additional simulations are needed to quantify the range of possibilities.

## Acknowledgements

The author is grateful to Anand Sivaramakrishnan and Joe Green for assistance with the interpretation of the predicted PSF of JWST; to Joe Green for providing the model PSFs used in the quantitative tests presented here; and to Gary Bernstein, Mike Fitzmaurice, Jerry Kriss, John Mather, Dave Redding, Jason Rhodes, Massimo Stiavelli, Peter Stockman, and Dave van Buren for many useful comments and discussions.

## References

- Bacon, D.J., Refregier, A., Clowe, D., & Ellis, R.S. 2001, MNRAS 325, 1065
- Barber, A.J., Thomas, P.A., Couchman, H.M.P., & Fluke, C.J. 2000, MNRAS 319, 267
- Bernstein, G., & Jarvis, M. 2002, AJ 123, 583
- Casertano, S., Griffiths, R.E., & Ratnatunga, K.U. 2001, in *Gravitational Lensing*, eds. Brainerd and Kochanek, ASP 237, p. 387
- Casertano, S., Ratnatunga, K.U., & Griffiths, R.E. 2002, in preparation
- Fischer, P., & Tyson, J.A. 1997, AJ 114, 14
- Green, J.J. 2002, private communication
- Griffiths, R.E., Casertano, S., Ratnatunga, K.U., & Im, M. 1996, MNRAS 282, 1159
- Jain, B., & Seljak, U. 1997, ApJ 484, 560
- Kaiser, N. 2000, ApJ 537, 555
- Kaiser, N., Squires, G., & Broadhurst, T. 1995, ApJ 449, 460
- Kuijken, K. 1999, AA 352, 355
- Maoli, R., et al 2001, A&A 378, 766
- Petro, L., et al. 2001, at <http://www.ngst.stsci.edu/nms/main/index.html>
- Schneider, P., & Seitz, C. 1995, AA 294, 411
- van Waerbeke, L., et al 2000, A&A 358, 30
- van Waerbeke, L., et al 2001, A&A 374, 757
- Wilson, G., Kaiser, N., Luppino, G.A., & Cowie, L.L. 2001, ApJ 555, 572

## Acronyms

- DRM:** Design Reference Mission
- ISIM:** Integrated Science Instrument Module
- JWST:** James Webb Space Telescope
- NGST:** Next Generation Space Telescope
- NMS:** NGST Mission Simulator
- OTE:** Optical Telescope Element
- PSF:** Point Spread Function
- S/N:** Signal-to-noise ratio
- WSC:** Wavefront Sensing and Control